

SOME ILLUSTRATIONS OF STOCHASTICITY

L. Jackson Laslett

University of California Lawrence Berkeley Laboratory
Berkeley, California*

A complex, and apparently stochastic, character frequently can be seen to occur in the solutions to simple Hamiltonian problems. Such behavior is of interest, and potentially of importance, to designers of particle accelerators -- as well as to workers in other fields of physics and related disciplines. Even a slow development of disorder in the motion of particles in a circular accelerator or storage ring could be troublesome, because a practical design requires the beam particles to remain confined in an orderly manner within a narrow beam tube for literally tens of billions of revolutions. The material I shall present is primarily the result of computer calculations I and others have made to investigate the occurrence of "stochasticity," and is organized in a manner similar to that adopted for presentation at a 1974 accelerator conference.¹

As an introductory example, one can consider the longitudinal motion of a particle subjected to the radio-frequency electric fields employed to bunch, and sometimes accelerate, a beam within a synchrotron type of accelerator. If the electric field is regarded as equivalent to a simple travelling wave, having the speed of a reference particle in a "coasting beam," the motion is characterized by the pair of differential equations.

$$\frac{dy}{dn} = -K \sin \pi x \quad (1a)$$

$$\frac{dx}{dn} = \lambda' y \quad (1b)$$

wherein y - fractional departure of energy from the reference value,

πx = electrical phase angle of field vs. particle,

$K \propto$ applied voltage, and

$\lambda' \propto$ derivative of revolution period with respect to energy.

NOTICE

This report was prepared as an account of work sponsored by the United States Government. Neither the United States nor the United States Department of Energy, nor any of their employees, nor any of their contractors, subcontractors, or their employers, makes any warranty, express or implied, or assumes any legal liability of responsibility for the accuracy, completeness or usefulness of any information, apparatus, product or process disclosed, or represents that its use would not infringe privately owned rights.

* Work supported by the U.S. Dept. of Energy, Office of Energy Research. *EB*

K and λ' will be regarded as specified constants. The differential equations will be recognized as derivable from a Hamiltonian function

$$H = \frac{1}{2} \lambda' y^2 - \frac{K}{\pi} \cos \pi x, \quad (2)$$

in which the independent variable (n) is the revolution number and does not appear explicitly in the Hamiltonian. Because n does not appear explicitly, the Hamiltonian of course is a constant of the motion. One accordingly obtains simple phase trajectories (in x,y space) -- of the familiar type characteristic of a physical (non-linear) pendulum (as was recognized by McMillan in connection with discovery of the principle of phase stability⁴).

In practice, however, the radio-frequency fields in fact are provided by localized cavities, so that the travelling-wave description constitutes an idealization and the motion is more appropriately represented by difference equations:

$$y_{n+1} = y_n - K \sin \pi x_n \quad (3a)$$

$$x_{n+1} = x_n + \lambda' y_{n+1}, \quad (3b)$$

with y_n measuring energy at the entrance to the n^{th} cavity. These transformation equations are readily shown to be area preserving [$\partial(x_{n+1}, y_{n+1}) / \partial(x_n, y_n) = 1$] -- the motion in fact could be described through use of a Hamiltonian function, but one that would contain a periodic δ -function of the independent variable as a factor multiplying the term $-\frac{K}{\pi} \cos \pi x$. There thus is no evident simple constant of the motion, and the non-linearity of the equations precludes application of Floquet theory to this problem. (The use of a Hamiltonian formulation nonetheless can be helpful in analytic work, but difference equations of course are convenient for computational investigations.)

It is of interest to take a quick look at some computational results obtained through use of a transformation equivalent to (3a,b) but written in

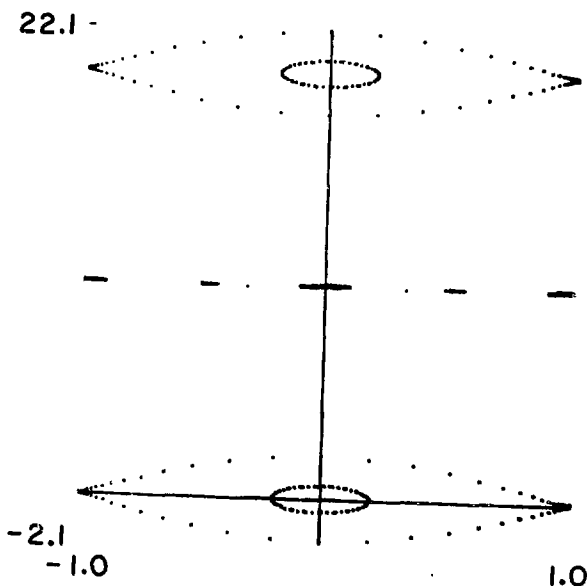
terms of working variables $Y = y - (K/2) \sin\pi x$, $X = x$, so that the transformation assumes the form

$$X_{n+1} = X_n + \lambda' [Y_n - (K/2) \sin\pi X_n] \quad (3a')$$

$$Y_{n+1} = Y_n - (K/2) [\sin\pi X_n + \sin\pi X_{n+1}] \quad (3b')$$

with the result that the resulting phase diagrams will necessarily have a desirable symmetry about both the X- and Y-axes. With $K/\pi = 0.1$ and $\lambda' = 0.1$ we find what appear to be conventional bucket diagrams with buckets separated in Y by $2/\lambda'$ for successive harmonic modes, although we may wish to return to the question of whether the bucket boundaries are as simple and definite as appears on Fig. 1.

RF Phase Plot $K/\pi = 0.1$
 $\lambda' = 0.1$



XBL 744-741

Fig. 1 -- X, Y phase plot for a coasting beam under the influence of an R.F. cavity with $K/\pi = 0.1$, $\lambda' = 0.1$ -- as computed by Eqns. (3a', b'). X is plotted mod. 2.

We also find evidence of some "sub-harmonic" structure (with higher order fixed points) that, if enlarged some 60X, has the appearance shown in Fig. 2.⁵

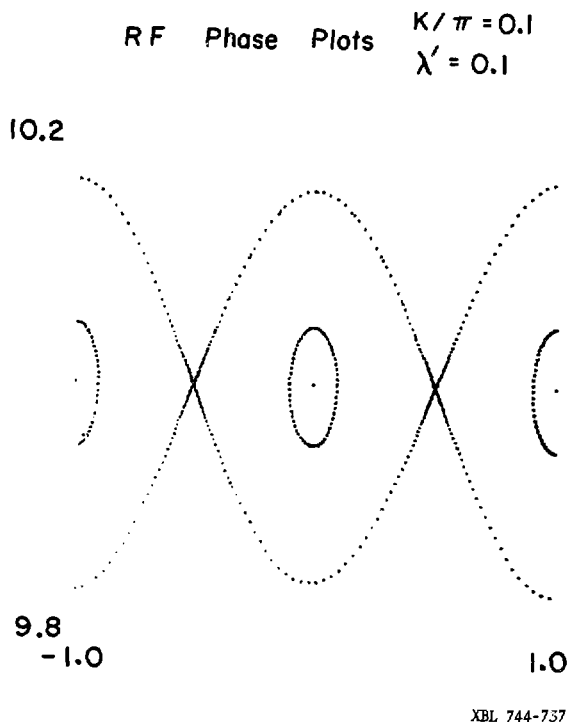


Fig. 2 -- Circa 60-fold vertical enlargement of central portion of Fig. 1, near $Y = 10.0$, showing sub-harmonic structure.

If the cavity voltage is increased eight-fold (so $K/\pi = 0.8$), the bucket areas are expected to become larger, and we indeed find this to be the case (Fig. 3), with an accompanying very marked increase of complexity

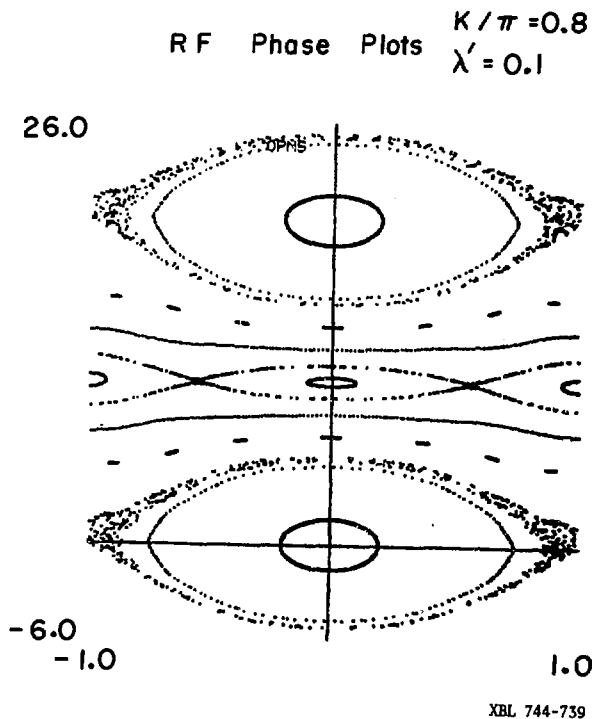


Fig. 3. - Phase plot similar to Fig. 1, but for operation with $K/\pi = 0.8$, showing the obvious development of complex structure.

that is immediately apparent in the phase plot. Of particular interest is the evident diffuse character of phase trajectories generated by points launched close to the first-order unstable fixed points situated at $X = \pm 1$, since the bucket boundary in consequence no longer appears clearly defined.

In the first example ($K/\pi = 0.1$), on the other hand, where the bucket width is some two and one-half times smaller in relation to the bucket separation, the presence of structure in the separatrix can be revealed computationally only with considerable care.⁶ To do this, one can extend from the unstable fixed points the eigenvector directions of the transformation linearized about these fixed points, and examine whether such curves intersect

smoothly. One finds in fact that they do not quite do so, but generate loops (of a nature to be illustrated later) that in this instance ($K/\pi = 0.1$) have a very small area that amounts to only about $1/(5 \times 10^{11})$ of the area of the bucket itself.

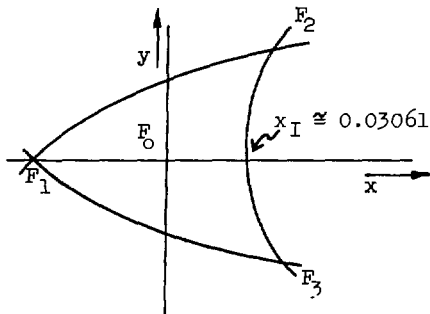
Another example of a "time-dependent" non-linear problem in the phase plane arose in connection with the development of spiral-sector fixed-field accelerators (as have now evolved into very effective cyclotrons for physical research). The equations for particle motion in these devices again required a time-dependent Hamiltonian and were distinctly non-linear. The limitations of computer performance at that time (1956) understandably motivated us to study the behavior of simple algebraic transformations that at least would duplicate approximately the short-term particle motion. Such an area-preserving transformation is

$$x_{n+1} = Ax_n \pm (1 - A^2)y_n + (1 - A) [x_n \pm (1-A)y_n]^2 \quad (4a)$$

$$y_{n+1} = \mp x_n + Ay_n \pm [x_n \pm (1-A)y_n]^2, \quad (4b)$$

where the \pm signs refer to the forward or inverse transformation, respectively, and A represents the cosine of the phase advance per iteration for solutions to the linearized (small-amplitude) transformations. The constant A normally would be taken to have an absolute value less than unity and, to avoid a one-third resonance when the quadratic terms are present, one also should avoid the value $A = -1/2$ (for which $\cos^{-1} A = 2\pi/3$).

The region of interest to the accelerator designer at that time is that contained within the roughly triangular area indicated on Fig. 4, sketched for $A = -5/8$ [$\cos^{-1} A \cong (0.35745)(2\pi)$], wherein the apparent separatrices through the fixed points F_1, F_2, F_3 are associated with the $2/3$ resonance and also illustrate the symmetry of the transformation (4a,b) with respect to the x -axis. It was only by rather careful computations [aided by Mrs. H. (Barbara) Levine -- see Ref. 12] that I could establish that the trajectories extending from the fixed points F_1, F_2, F_3 do not intersect smoothly and hence give rise to (rather modest) regions of erratic behavior similar to those seen in phase diagrams for the earlier example. Outside the area F_1, F_2, F_3 indicated in Fig. 4, however,



Sketch for $A = -5/8$

$$\cos^{-1}A \cong (0.35745)(2\pi)$$

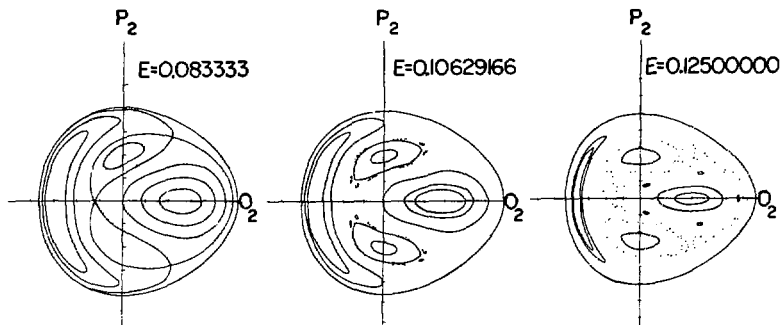
Area $\cong 5.5 \times 10^{-3}$
 (would shrink to zero
 if $A \rightarrow -1/2$)

$$F_1: \left(-\frac{\sqrt{41-5}}{26}, 0\right) = (-0.053966\dots, 0)$$

$$F_{2,3}: \left(\frac{1}{26}, \pm \frac{4\sqrt{41-16}}{169}\right) = (0.03846\dots, \pm 0.05688\dots)$$

XBL 7712-11142

Fig. 4 - Apparent separatrices through the third-order unstable fixed points of the transformation (4a,b), with $A = -5/8$.



XBL 744-740

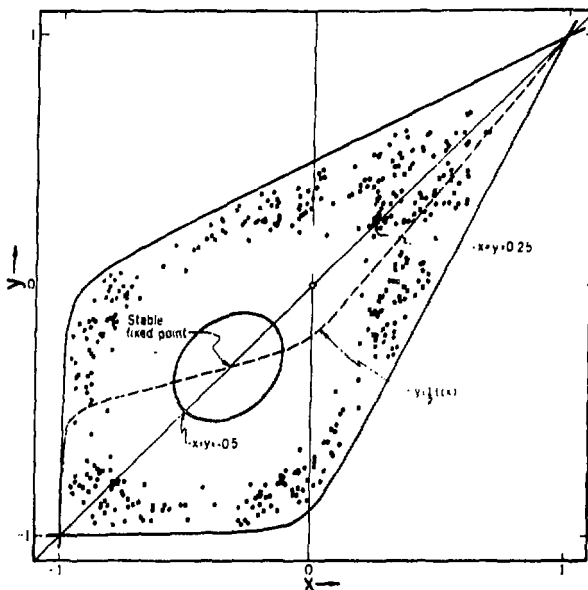
Fig. 5 - Phase plots, in the surface of section $q_1 = 0$, resulting from the equation implied by the Hamiltonian function (5) -- for increasing values of the energy. [After Walker and Ford.⁸]

the transformation (4a,b) develops gross loops in phase trajectories extending from an order-1 fixed point at (1,0), and in this respect exhibits a behavior similar to that shown by a transformation of deVogelaere which will be mentioned later.

Similar questions concerning the character of phase trajectories and the possible erratic or stochastic behavior of canonical mappings can arise in problems with more than one degree of freedom. As an example, Hénon and Hiles⁷ and subsequently Walker and Ford⁸ studied a model of an astronomical system, for which the Hamiltonian function was taken to be

$$H = \frac{1}{2}(p_1^2 + p_2^2 + q_1^2 + q_2^2) + q_1^2 q_2 - \frac{1}{3} q_2^3. \quad (5)$$

The cubic terms appearing here as coupling terms become increasingly significant for increasingly large values of H -- which is itself a constant of the motion. With the coupling terms present, however, and in the absence of any simple constant of the motion other than H, a given phase trajectory might be expected to wander (ergodically) over virtually all of a three-dimensional surface specified by $H = \text{Constant}$ (and that will be a closed surface for values of H below the dissociation energy). If, on the other hand, some additional integral of the motion were in fact also acting, the phase points of a given trajectory then would be constrained to lie on a two-dimensional surface, and graphs of the intersection of such surfaces with some selected plane or other surface (a "surface-of-section") would lead to simple curves in this plane rather than to a scattering of points. Computations of this nature indicated that for sufficiently small values of energy (e.g., $H \leq 1/12$) only curves that to computer accuracy were smooth (and relatively simple) were formed by intersection with the plane $q_1 = 0$ (and $p_1 > 0$). Examples in which the energy of the particles was successively raised, however, resulted in the development of ragged island structures or of apparent stochastic behavior over increasingly large portions of this surface-of-section (Fig. 5).



XBL 744-684

Fig. 6 - Phase diagram for the transformation (6a, b), with $f(y)$ given by Eqn. (7a). The scattered points result from computations initiated with $x_0 = y_0 = 0.25$, but must remain within the separatrix defined by the function ϕ [Eqn. (7b)]. $k = 0.1$.

Such behavior appears concordant with the "KAM" (Kolmogorov-Arnol'd-Moser) theory (see Ref. 58, 59. & 60 of our Ref. 2c), which suggests that many of the invariant curves or surfaces present in the absence of the perturbation will persist, with only minor distortion, in the presence of a sufficiently small perturbation (see, however, Note 9). It is of interest, of course, to determine or to estimate the circumstances (e.g., perturbation strength) at which the KAM theory becomes inapplicable and extended regions of erratic (or stochastic) behavior develop. As we suggested by our first examples, and has been expounded more extensively by Zaslavskij and Chirikov,^{2c,10} one means for obtaining such estimates may be by determining the ratio of resonance width $[\delta\omega=(d\omega/dI)_r\delta I]$ to the distance ($\Delta\omega$) to the nearest neighboring resonance.

Additional tests (to be mentioned below) may be required to determine the degree of disorder associated with the movement of phase points in such

stochastic regions. We may first note, however, that the existence of nested closed invariant curves in a plane -- as suggested by the KAM theorem for a problem in one degree of freedom -- prevents phase points from moving outward or inward to regions of substantially different "amplitude" (in the absence of noise). With more than one degree of freedom, however, stochastic layers may intersect, to form an intricate system of channels along which a phase point can slowly diffuse and result in instability. The possibility of such "Arnol'd diffusion" has been demonstrated by Arnol'd [Ref. 35 of our Ref. 2c; stated simply the example considered by Arnol'd is comprised of a physical pendulum and a simple-harmonic oscillator, with a time-dependent coupling (that also depends on the phases, or angle variables, of these oscillations)].

It should be pointed out that some non-linear transformations -- say for a system with one degree of freedom -- will not lead to the disappearance of some or all of the invariant phase curves at substantial amplitudes. Thus for transformations of the form

$$x_{n+1} = y_n; y_{n+1} = -x_n + f(y_n), \quad (6a,b)$$

McMillan¹¹ has shown that if $f(y)$ can be written as $\phi(y) + \phi^{-1}(y)$ (where ϕ^{-1} denotes the function inverse to ϕ), then the curves $y = \phi(x)$ and $x = \phi(y)$ will constitute invariant curves. Such curves will pass through the first-order fixed point(s) situated at the intersection(s) of $y = (1/2)f(x)$ with the principal diagonal. An enclosed area can thereby be formed from which phase points cannot escape even if the behavior in portions of the interior becomes highly stochastic. This is illustrated by an example (Fig. 6) in which

$$f(y) = \frac{1}{2}(3y-1) - \frac{1}{2} \frac{k^2}{y+1} + \sqrt{y^2 + k^2} \quad (7a)$$

and

$$\phi(x) = x - 1 + \sqrt{x^2 + k^2} \quad (7b)$$

Such a situation also can develop when $f(y)$ is a stepwise linear function of y with discontinuities of slope, as has been noted by Drs. Judd and

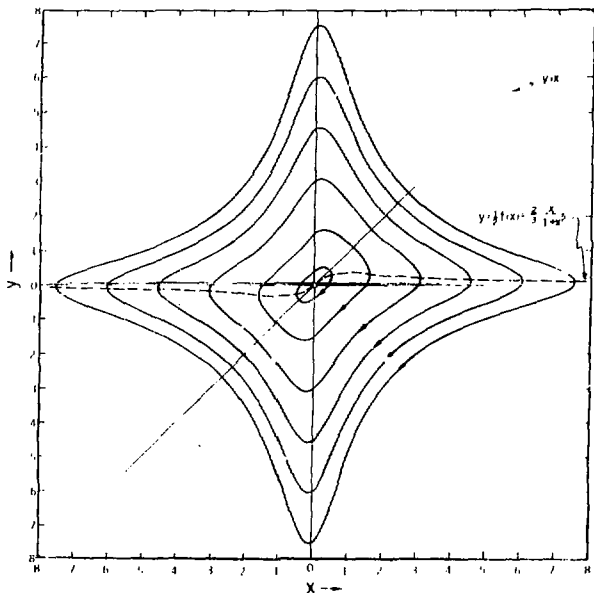
McMillan [see, for example, Figs. 13 and 14 (pp. 27-28) of Ref. 12]. If $f(y)$ is of the form

$$f(y) = -(By^2 + Dy)/(Ay^2 + By + C), \quad (8)$$

moreover, the entire phase plane will be covered by a family of simple invariant curves -- see, for example, the cases¹¹ $f(y) = 2ky/(1+y^2)$, with the invariants $x^2y^2 + x^2 + y^2 - 2kxy = \text{Constant}$, and $f(y) = 2ky/(1-y^2)$, with the invariant: $x^2y^2 - x^2 - y^2 + 2kxy = \text{Constant}$, illustrated by Figs. 7-8.

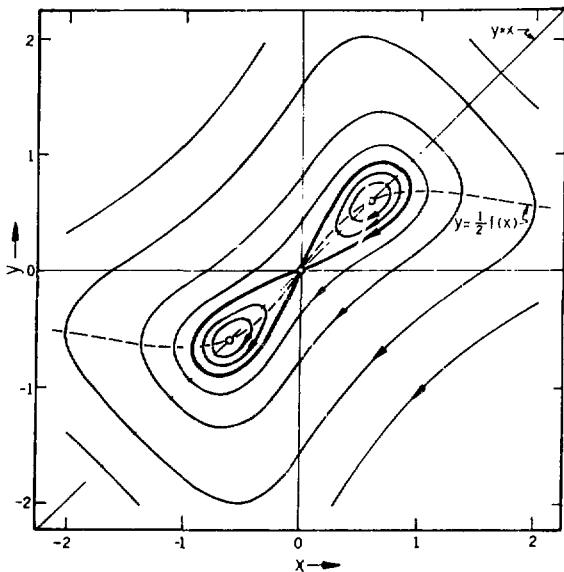
It is of interest to examine the mechanism whereby irregular behavior can develop in the neighborhood of unstable fixed points, taking as an illustration an example suggested by Professor deVogelaere that [when generalized and re-written in variables leading to the form (6a,b) advocated by McMillan] employs

$$f(y) = 2[Ty + (1 - T)y^2]. \quad (9)$$



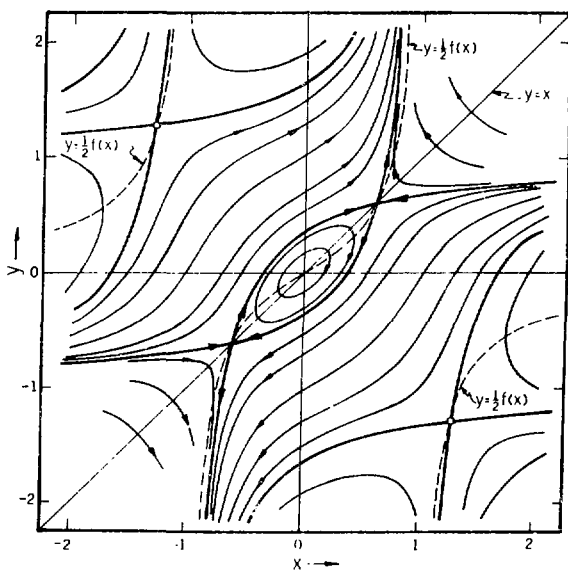
XBL 744-680

Fig. 7 - Invariant curves for the transformation (6a, b) with $f(y) = 2ky/(1+y^2)$ and $k = 2/3$. [Figs. 7 - 11 after McMillan.¹¹]



XBL 744-681

Fig. 8 - Invariant curves for the same transformation as in Fig. 7, but with $k = 1.36$.



XBI. 744-682

Fig. 9 - Invariant curves for the transformation (6a, b) with $f(y) = 2ky/(1-y^2)$ and $k = 0.64$.

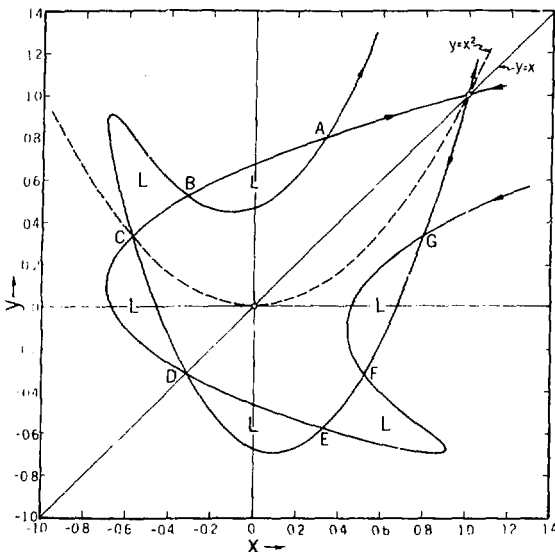


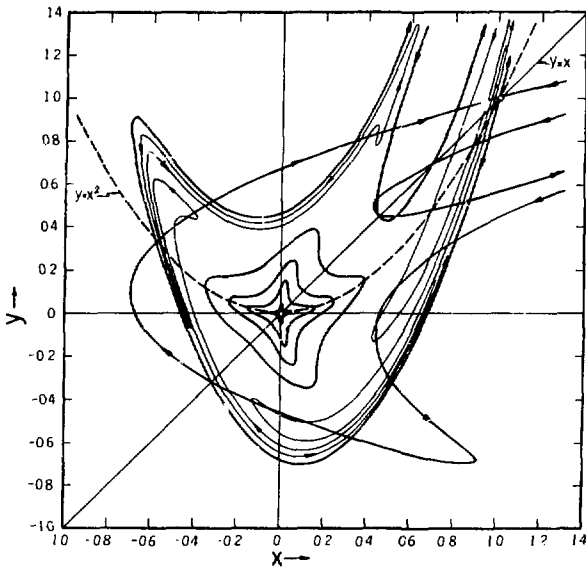
Fig. 10 - Plot of the extensions of the eigenvector directions from the unstable fixed point at $(1,1)$, for the deVogelaere transformation expressed in McMillan's variables [Eqns. (6a, b) and (9), with $T = 0$]. The areas of the loops marked L are all equal, by virtue of the area-preserving character of the transformation and the inherent symmetry about the principal diagonal.

First-order fixed points appear at $(0,0)$ and at $(1,1)$. For $T = 0$, this transformation, when linearized about the unstable fixed point at $(1,1)$, can be represented by the matrix $\begin{matrix} 0 & 0 \\ -1 & 4 \end{matrix}$, with eigenvalues and eigenvector slopes

$$\lambda = 2 \pm \sqrt{3}, \quad dy/dx = \lambda.$$

A line segment extending downward from the fixed point $(1,1)$ with the slope $2 + \sqrt{3}$, if subjected to repeated applications of the transformation, generates the loops shown in Fig. 10; similarly a line segment of slope $2 - \sqrt{3}$, if extended by the inverse transformation, generates the mirror-image curve (mirrored about the principal diagonal). Points such as A, B, C ... progress toward the fixed point in smaller and smaller steps and, since the transformation is area-preserving, the associated loops clearly must become increasingly elongated as they become increasingly narrow from repeated applications of the forward transformation. The evolution of such loops clearly will become quite intricate (Fig. 11), but the loops apparently need not permeate the entire

"interior". Portions of an inward loop can, in fact, enter, on a later iteration, into the interior of an outward-lying loop, as indicated on Fig. 11. A wealth of island structure, of course, can develop throughout the area of such phase diagrams.



XBL 744-679

Fig. 11 - A partial extension of the curves shown on Fig. 10.

In some instances a family of unstable fixed points for which the eigenvalues are negative may arise (in place of a stable family, for which λ is purely imaginary), and the appearance of phase trajectories can thereby be drastically affected. Phase trajectories in the neighborhood of two such eighth-order ("tune" = 2/3) fixed points are shown on Fig. 12 for the transformation of deVogelaere written to exhibit symmetry about the x-axis

$$x_{n+1} = y_n + Tx_n + (1-T)x_n^2 \quad (10a)$$

$$y_{n+1} = -x_n + Tx_{n+1} + (1-T)x_{n+1}^2, \quad (10b)$$

with $T = -1/3$. In any case it is clear, however, that the development of a loop system such as that shown on Fig. 11, can readily give rise to an apparent stochastic motion of phase points in portions of the phase diagram -- most particularly near an unstable fixed point.

The existence of a firm separatrix, or of an extensive family of invariant curves generally, can be extremely sensitive to the exact form of the transformation.¹⁴ A case of some physical interest arises in computational studies relating to the Toda Lattice.¹⁵ This one-dimensional lattice consists of particles interacting through exponential pair potentials and can propagate certain nonlinear wave forms ("solitons") without change of shape. One computational investigation¹⁶ of stability for a three-particle lattice (with periodic boundary conditions) has commenced with a Hamiltonian function

$$H = \frac{1}{2}(p_1^2 + p_2^2 + p_3^2) + e^{-(q_1 - q_3)} + e^{-(q_2 - q_1)} + e^{-(q_3 - q_2)}. \quad (11)$$

By a canonical transformation of variables, in recognition of the invariance of

this system to translation -- so that $I_1 = P_1 + P_2 + P_3$ constitutes a constant of the motion -- the Hamiltonian (11) becomes expressible as a function of two pair of conjugate variables in the form

$$H = \frac{1}{2}(p_1^2 + p_2^2) + \frac{1}{24} [e^{(2q_2+2\sqrt{3}q_1)} + e^{(2q_2-2\sqrt{3}q_1)} + e^{-4q_2}], \quad (12)$$

which is identical to the Hénon-Heiles Hamiltonian function (5) through terms of third order. It is of interest to examine whether in the present case constants of the motion other than H act to restrict the motion. Computationally it was found -- again using the surface-of-section $q_1 = 0 (p_1 > 0)$ -- that in this case simple invariant curves apparently continue to exist in the $q_2 p_2$ plane, even for very large values of H . Stimulated by this result, Hénon¹⁷ has directed attention to an additional integral of the motion that is valid in this case; the constants of the motion for the three-particle lattice then can be written in a form that we may express as¹⁸

$$H = \text{Constant} \quad (13a)$$

$$P_1 + P_2 + P_3 = \text{Constant, and} \quad (13b)$$

$$P_1 P_2 P_3 - P_1 e^{-(Q_3-Q_2)} - P_2 e^{-(Q_1-Q_3)} - P_3 e^{-(Q_2-Q_1)} = \text{Constant.} \quad (13c)$$

Evidently¹⁷ further analytic work in fact has now established that the n -particle Toda lattice with periodic boundary conditions (or with fixed ends) is a "completely integrable" system.

It is of some interest to seek means for anticipating whether stochastic behavior will occur in various portions of a phase diagram and to examine the character of such stochastic behavior as does occur. What we here have loosely termed stochastic behavior can be catalogued with respect to a hierarchy of properties (ergodicity, mixing, ...), indicative of increasing disorder, that are fundamentally significant for statistical mechanics.^{2a,e} Of particular interest to the accelerator designer, of course, is the determination of a threshold beyond

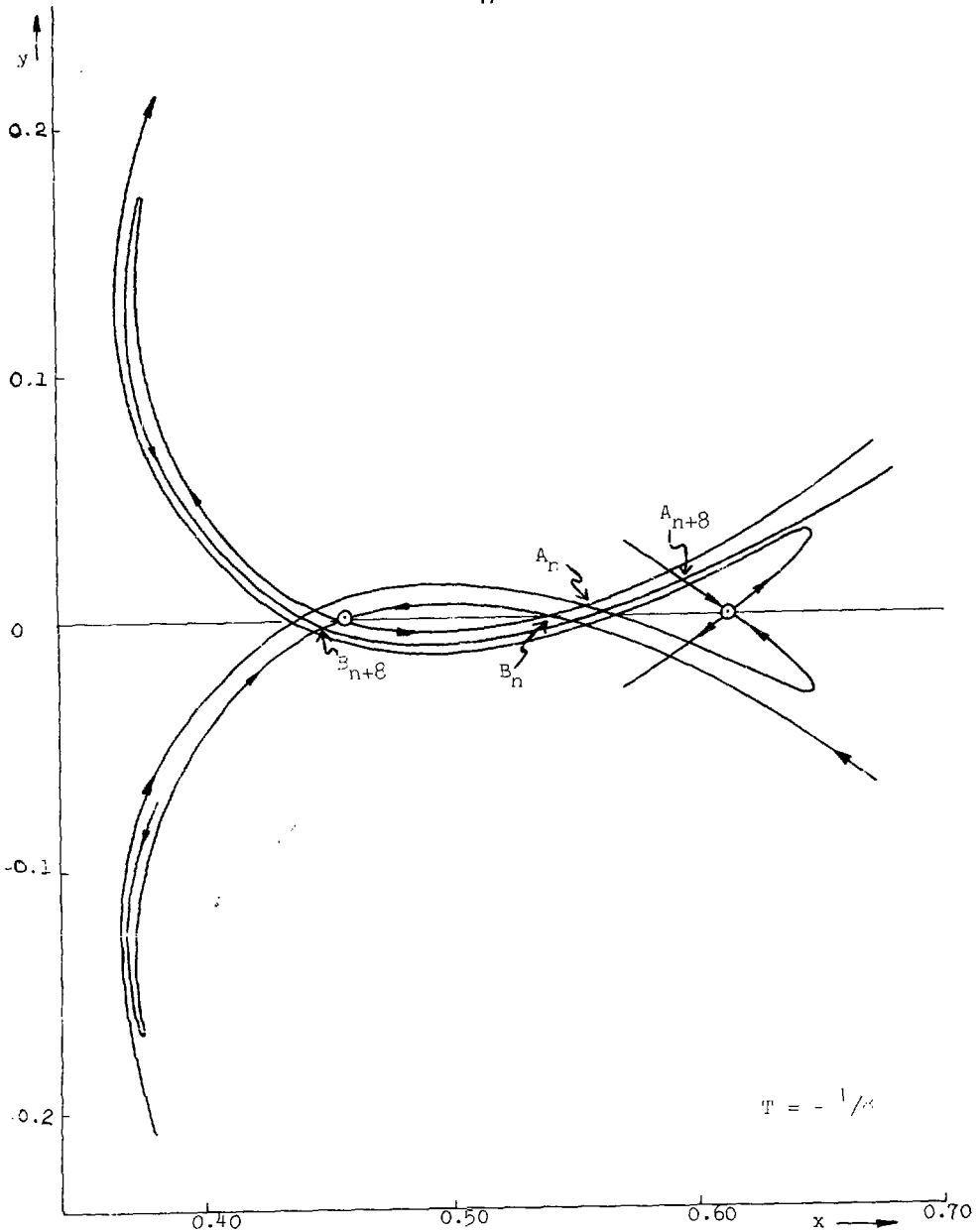


Fig. 12 - Phase trajectories for the transformation (10a,b) with $T = -1/8$, in the neighborhood of two fixed points for which the eigenvalue is negative.

which stochastic behavior will set in and may act to carry a phase point to unacceptably large amplitudes. As noted earlier, stochastic behavior appears to be associated with overlapping resonances,^{2c} and this concept has served as the basis for some analytic estimates of stochasticity limits.^{2c,19} It has been noted by René deVogelaere and confirmed in subsequent computations²⁰ that for a particular class of fixed-point families -- say those with rotation of the form $m/(4m+1)$ -- there is a closely linear relationship between the order of the resonance $(4m+1)$ and $\ln|1 - \frac{1}{2} \text{Trace}|$ through many decades ("Trace" denoting the trace of the tangential-mapping or differential matrix associated with the $4m+1$ iterations required to map a given fixed point onto itself). Such regularities, and others relating to the apparent size of the stable areas about high-order fixed points (e.g., as estimated from the intersection angle of eigenvectors), have been considered useful indicators of the change in character of a mapping at certain amplitudes.^{21,10,22}

A computational procedure of considerable interest for recognizing stochasticity is that in which one follows the evolution of the distance between two initially very close points in phase space. In practice it can prove desirable to reduce the separation from time to time by a recorded factor whenever the separation becomes excessive during the computations, or, perhaps preferably, to evaluate the growth of an infinitesimal vector through use of the cumulative tangential-mapping matrix. A high degree of stochasticity can be ascribed to the behavior of the transformation if there are such vectors whose length generally grows beyond the first iteration by a factor greater than unity (while others may similarly contract). (Ref. 2a, p. 55; for examples, see Ref. 23.) An analogous procedure -- that can be more attractive, although possibly of a less direct basic significance -- is an investigation of the growth of the eigenvalue(s) of the cumulative tangential mapping. Such eigenvalues can change sign repeatedly during the course of many iterations, and hence will be seen to decrease from

time to time, but an exponentially increasing trend in eigenvalue magnitude is likely to be associated with a similar type of increase for the lengths of the vectors mentioned previously. The nature of eigenvalue growth has been illustrated by Froeschlé²⁴ for the transformation²⁵

$$x_{n+1} = x_n \cos \alpha - (y_n - x_n^2) \sin \alpha \quad (14a)$$

$$y_{n+1} = x_n \sin \alpha + (y_n - x_n^2) \cos \alpha \quad (14b)$$

The general characteristics of this transformation, expressed in variables such that the transformation has the symmetry of McMillan's form, is seen on Fig. 13. On an expanded scale (X10), we see (Fig. 14) the sudden onset of erratic behavior as the starting values for the transformation are successively increased (in steps $\Delta x_0 = 0.0025$, for $y_0 = 0$), and on a scale expanded by a further factor 100/6 we see (Fig. 15) the presence of a great deal of additional structure within a portion of this "stochastic" region. Associated with the transition to the stochastic region there appears to be a marked change in the manner of growth of $\psi_n = \log|\lambda_n|$ (linear, vs. n , in the stochastic case -- indicative of an exponential trend for $|\lambda_n|$) or of the "Cesaro

mean" $\mu_n = \frac{1}{n} \sum_{m=1}^n \frac{1}{m} \psi_m$ (constancy in the stochastic case, monotonically decreasing

otherwise -- Fig. 16).²⁶ Such methods indeed may prove useful in investigating computationally the possible development of stochastic motion in storage-ring devices. Extended computations of this nature can present challenging problems with respect to computer accuracy.²⁷



XBB 744-2448

Fig. 13 - Apparently smooth phase curves and a scattering of points resulting from iteration of the transformation (14a,b), with $\cos \alpha = 0.22$ and coordinates X, Y appropriate to expressing the transformation in the form (6a,b).²⁵ Five islands of stability (containing stable fixed points of order 5) are seen surrounding the area associated with the order-1 fixed point at the origin. The outermost smooth curve, shown as bounding this inner area, resulted from the starting values $x_0 = 0.5350, y_0 = 0$ (Froschlé notation), and the scattered points result from $x_0 = 0.5375, y_0 = 0$. Scale (as indicated by the coordinate axes): -1.0 to 1.0



XBB 744-2446

Fig. 14 - Enlarged portion (10X) of Fig. 13, showing seven smooth phase trajectories resulting from starting values $x_0 = 0.5200, 0.5225, \dots, 0.5350$ (and $y_0 = 0$) and a scattering of points resulting from $x_0 = 0.5375, y_0 = 0$. Note the occurrence of open areas within the region covered by the scattered points -- for example the area surrounding an (unplotted) stable fixed point of order 65 at $X \cong 0.476, Y \cong 0.521$
Scale: 0.38 to 0.58



XBB 744-2447

Fig. 15 - Detailed multiple-island structure in the immediate neighborhood of an order-65 stable fixed point (shown here just below the center of the diagram) of which mention has been made in the caption to Fig. 14.
Scales: 0.470 to 0.482 for X, 0.516 to 0.528 for Y.

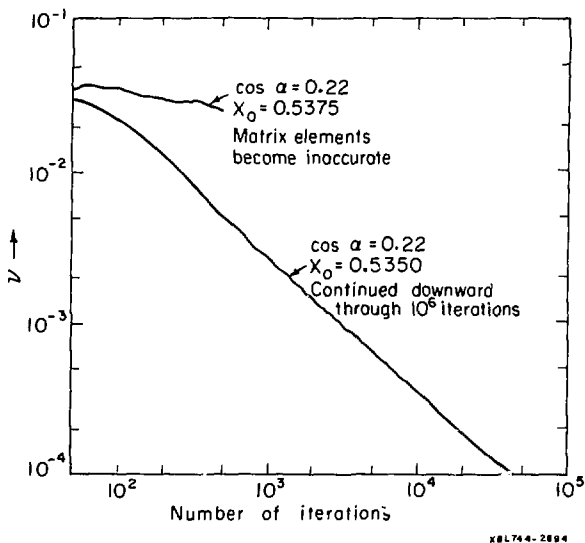


Fig. 16 - Plots of the "sliding mean", v_n (Note 26), vs. n , obtained from computations begun (i) with initial conditions leading to the last smooth curve of Fig. 14 ($x_0 = 0.5350$) and (ii) with initial conditions leading to the scattered points on that Figure ($x_0 = 0.5357$), of which only the results for the latter case indicate a general exponential upward trend of $|\lambda_n|$.

REFERENCES AND NOTES

1. L. Jackson Laslett, "Stochasticity", Proc. IX International Conf. on High Energy Accelerators, Stanford Linear Accelerator Center, CONF 740522 (S.L.A.C., Stanford, Calif.; 1974), pp. 394 - 400.
2. (a) An authoritative treatment of the mathematical aspects of the problems discussed here is given by V.I. Arnol'd and A. Avez, "Ergodic Problems of Statistical Mechanics" (Benjamin, New York, N.Y.; 1968) and (b) by Jürgen Moser, "Stable and Random Motions in Dynamical Systems" (Princeton Univ. Press, Princeton, N.J.; 1973); (c) an extended discussion of which portions relate more immediately to those of interest to an accelerator designer is presented, with many references, by G.M. Zaslavskij and B.V. Chirikov, Uspekhi Fizicheskikh Nauk 105 and Engl. Transl. Sov. Phys. Usp. 14, 549-568 (1972), with further discussion and examples (d) by B.V. Chirikov in Nucl. Phys. Inst. Report 267 (Novosibirsk, USSR) with Engl. Transl. by A.T. Sanders, CERN Trans. 71-40 (CERN, Geneva, Switzerland; October 1971); and (e) related questions of ergodic theory in statistical mechanics are summarized by J.L. Lebowitz and O. Penrose, Physics Today, pp. 23 - 29 (February 1973).
3. CNRS Internat. Conf. on Point Transformations and their Applications, Laboratoire d'Automatique et d'Analyse des Systèmes Toulouse, France (10-14 September 1973). This conference was concerned with both Hamiltonian and non-Hamiltonian systems.
4. E.M. McMillan, Phys. Rev. 68, 143-144 (1945).
5. K.R. Symon and A.M. Sessler, Proc. CERN Symposium on High Energy Accelerators and Pion Physics 1, 44-58 (CERN, Geneva, Switzerland; 1956).

6. L. Jackson Laslett, ERAN-57 (Lawrence Berkeley Laboratory; 1970).
7. M. Henón and C. Heiles, *Astron. J.* 69, 73-79 (1964).
8. G.H. Walker and J. Ford, *Phys. Rev.* 188, 416-432 (1969).
9. The present example in fact is exceptional in that the unperturbed frequencies, being equal, are "rationally connected" and the analysis requires special treatment -- see F.G. Gustavson, *Astron. J.* 71, 670-686 (1966); J. Moser, "Lectures on Hamiltonian Systems", *Memoirs Amer. Math. Soc.*, No. 81, 1-60 (1968).
10. See also *Vestnik Mekhaniki*, *Soviet Math.* 4, 200-270 (1963).
11. Edwin M. McMillan, "A Problem in the Stability of Periodic Systems", in "Topics in Modern Physics -- A Tribute to Edward U. Condon", pp. 219-244 (Colorado Assn. University Press, Boulder, Colorado; 1971). A transformation written in the form (6a,b) is convenient for the study of area-preserving transformations in the plane because of the "double symmetry" pointed out by McMillan (p. 225). The transformation can be interpreted as describing the effect of a simple linear focusing system supplemented by a periodic sequence of thin non-linear lenses that introduce at such points a Δy specified by $f(x)$.
12. Laslett, McMillan, and Moser, Courant-Institute Report NYO-1480-101 (New York University, N.Y.; 1 July 1968).
13. Fig. 12 is taken from Fig. 2 (p. 35) of the Appendix to Ref. 12. The fixed points shown are situated on the x-axis at $x \cong 0.4562733$ and 0.6130793 , with the negative eigenvalue $\lambda \cong -8.369$ (in addition to its reciprocal, $\lambda \cong -0.1195$) for this family, and the point A_{n+8} is the eighth iterate of point A_n . For discussion of the occurrence and consequences of loop systems, see S. Smale, "Diffeomorphisms with Many Periodic Points ...", (Princeton University Press, Princeton, N.J.; 1965); E. Zehnder, *Comm. Pure Appl. Math.* 26, 131-182 (1973); Ref. 2c, Sect. 6.1; and Ref. 2d, Sect. 2.6.

14. The loss of a firm separatrix can be illustrated computationally for the transformation (6a, b) by modifying the function $f(y)$ of (7a) so as to introduce the quantity $1 - b$ as a factor multiplying the second term on the right and setting $b \neq 0$ (for example, $b = 0.05$) -- L. Jackson Laslett, ERAN-239 (1974).
15. See, for example, M. Toda, Prog. Theoret. Phys. (Kyoto) Suppl. 45, 174-200 (1970); references cited therein; and related papers in this issue of the Supplement.
16. J. Ford, S.D. Stoddard, and J.S. Turner, Prog. Theoret. Phys. (Kyoto) 50, 1547-1560 (1973).
17. Cited in Ref. 16, p. 1558.
18. The validity of these (time-independent) expressions as constants of the motion of course can be confirmed directly by forming their Poisson-bracket expressions with the Hamiltonian function (11).
19. B.V. Chirikov, E. Keil, and A.M. Sessler, CERN Report ISR-TH/69-59 (CERN, Geneva, Switzerland; 15 October 1969).
20. E.g., Ref. 12, pp. 42-43, where is also listed a quantity $\lambda_I = \lambda - 1$ for fixed-point families that have rotation $\frac{m}{4m+1}$.
21. John M. Greene, J. Math. Phys. 9, 760-768 (1968).
22. James H. Bartlett, "Stability of Area-Preserving Mappings", Paper III-3 of Ref. 3.
23. J. Ford and G.H. Lunsford, Phys. Rev. A1, 59-70 (1970).
24. C. Froeschlé, Astron. and Astrophys. 9, 15-23 (1970); C. Froeschlé and J.P. Scheidecker, Ibid. 22, 431-436 (1973); and other references cited therein.
25. This transformation, (14a,b), can be put into McMillan's form¹¹ by the change of variables $x = \sqrt{\sin \alpha} Y$, $y = (X - Y \cos \alpha) / \sqrt{\sin \alpha}$, with $f(Y)$ then becoming $2Y \cos \alpha + Y^2 \sin^3/2\alpha$.

26. The curves of Fig. 16 are plots of

$$v_n \equiv \sum_{m=1}^n \frac{1}{m} \psi_m \exp\left(-\frac{n-m}{\tau}\right) / \sum_{m=1}^n \exp\left(-\frac{n-m}{\tau}\right) \text{ with } 1/\tau = 0.015, \text{ the}$$

sliding exponential factor being designed to provide some smoothing of the results (L. Jackson Laslett, unpublished LBL Report). Extended computations of this nature can present challenging problems with respect to computer accuracy.²⁷

27. C. Froeschlé and J.-P. Scheidecker, J. Comp. Phys. 11, 423-439 (1973);
Astrophys. & Space Sci. 25, 373-386 (1973).

28. I am deeply indebted to Paul J. Chanell for many stimulating and helpful conversations concerning topics discussed here. Responsibility for the views expressed in this paper, however, remains exclusively my own.